Journal of Visualization, Vol. 4, No. 3 (2001) 223-230

Visualization of Sudden-start Flow between Two Concentric Rotating Cylinders with Finite Length

Watanabe, T.*[1], Furukawa, H.*[2], Aoki, M.*[2] and Nakamura, I.*[3]

*1 Center for Information Media Studies, Nagoya University, Furo, Chikusa, Nagoya 464-8603, Japan.
e-mail: watanabe@info.human.nagoya-u.ac.jp
*2 Graduate School of Human Informatics, Nagoya University, Furo, Chikusa, Nagoya 464-8601, Japan.
*3 Department of Mechanical Engineering, Meijo University, Shiogamaguchi, Tempaku, Nagoya 468-8502, Japan.

Received 9 March 2001.
Revised 18 June 2001.

***Abstract*:** Numerical simulation and visualization are performed to investigate the developing processes of flows between two concentric rotating cylinders. The length of the cylinders is finite and the end walls are fixed. Initially the fluid is at rest, and the inner cylinder suddenly begins to rotate. Various flow modes appear in this flow. Developments of the flow to these modes are examined and the physical explanation for the transient process is presented. The processes are classified into some types. At low Reynolds numbers, vortices begin to grow on end walls. When the Reynolds number is higher, the centrifugal instability brings first vortices around the mid-plane in the axial direction. Some final modes are established via an intermediate mode, and some other modes are attained after merging and vanishing of vortices.

***Keywords*:** developing process of flow, Taylor-Couette flow, impulsive start, Ekman vortex, numerical simulation.

1. Introduction

Flow developing between a rotating inner cylinder and a stationary outer cylinder presents a major problem of a complex system which invokes bifurcation phenomena. When the aspect ratio defined by the quotient of the cylinder length by the gap width between cylinders is finite and the end walls of cylinders are fixed, the flow is more realistic and it has drawn considerable interests. Benjamin and Mullin (1981), for example, conducted experimental investigations and obtained flows of normal modes and anomalous modes. In the flow of an anomalous mode, an anomalous cell emerges near the end wall and the flow on the end wall is not inward but toward the outer cylinder. After their studies, researches were conducted mainly on the flow modes appearing in the fully developed flows (Koschmieder, 1993; Egbers and Pfister, 2000), and various modes were found experimentally and numerically (Nakamura et al., 1990; Nakamura and Toya, 1996).

The transient process of flow mode from an initial state at rest was studied from the viewpoint of the growth of Ekman cells appearing at stationary end walls of finite cylinders. Even at the Reynolds numbers less than the critical value for the onset of the Taylor vortex flow, the Ekman cell develops on the end wall. Lücke et al. (1984) focused on the flow with sudden increase in the rotating velocity and investigated the penetration process of the end-wall effect toward the mid-plane. Kuo and Ball (1997) calculated the case where the inner cylinder gradually began to rotate and showed the way in which vortices were formed near end walls. In these studies, the aspect ratio was not less than 10 and was not small, and the vortex which grew first was the one on the end wall. The experimental result of the time-dependent flow (Takeda et al., 1990), on the other hand, showed no evidence that the Taylor vortex flow would be induced by Ekman cells, and it was not consistent with the numerical results.

The number of cells may decrease during the formation process of the Taylor vortex flow. Bielek and Koschmieder (1990) investigated flows at low aspect ratios and determined the transient processes of flow patterns from observations. The molecular dynamics simulation by Hirshfeld and Rapaport (1998) reported the reduction of cells in the flow with a periodic condition in the axial direction. However, the aspect ratio and the Reynolds number were limited and the reduction process was not shown clearly.

We focus on the practical flows with a small aspect ratio of order of unity and study the flow modes appearing during and after the formation periods of flows. The rotating velocity of the inner cylinder suddenly changes from zero to a prescribed constant velocity. We visualize and investigate the transitions to quasi-steady states under various conditions, and clarify the types of the processes developing to various modes, which are difficult to be determined by experiments.

2. Formulation

Physical parameters are nondimensionalized by the reference length which is the gap between radii of cylinders and the reference velocity which is the maximum circumferential velocity of the inner cylinder. The radii of the inner cylinder and the outer cylinder are r_i and r_o, and the gap between them and the length of cylinders are D (=1) and L, respectively. The main parameters governing the flow are the aspect ratio $G = L/D$, the radius ratio $h = r_i/r_o$ and the Reynolds number *Re* defined by the reference length and the reference velocity.

The governing equations are the equation of continuity and the Navier-Stokes equations in the cylindrical coordinate system (r, q, z) shown in Fig. 1:

$$\nabla \cdot \boldsymbol{u} = 0, \tag{1}$$

$$\frac{\partial \boldsymbol{u}}{\partial t} + (\boldsymbol{u} \cdot \nabla)\boldsymbol{u} = -\nabla p + \frac{1}{Re}\nabla^2 \boldsymbol{u}, \tag{2}$$

where $\boldsymbol{u}$ is the velocity vector with the radial, circumferential and axial components u, v, w, and t is time and p is pressure. The pressure correction method is based on the Poisson equation

$$Dp = -\frac{\partial D}{\partial t} - \nabla \cdot ((\boldsymbol{u} \cdot \nabla)\boldsymbol{u}), \tag{3}$$

where D is the divergence of $\boldsymbol{u}$ and the viscous terms are neglected.

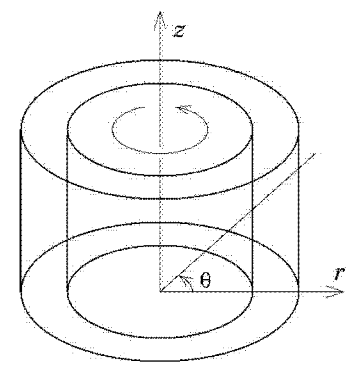

Fig. 1. Coordinate system.

The equations are discretized by the finite difference method. The convection terms are formulated by the secondary upwind scheme and other terms are represented by the central difference method.

The values of the velocity components in the initial condition are zero in the entire flow region. At time t = 0, the inner cylinder suddenly begins to rotate at a constant speed. The end walls of cylinders and the outer cylinder are not rotating and fixed. The boundary condition of the velocity components is the non-slip condition.

For the pressure Poisson equations, the Neuman condition which is evaluated from the pressure terms of momentum equations is used. The Poisson equations are usually solved by SOR, and ILUCGS is used when the reasonable convergence of the iterative method is not expected.

For the visualization of flows, Stokes's stream function y defined by

$$u = -\frac{1}{r}\frac{\partial y}{\partial z}, \qquad w = \frac{1}{r}\frac{\partial y}{\partial r}, \tag{4-a,b}$$

and the average of the kinetic energy in the meridional section with an area A, which is given by

$$E = \frac{1}{A}\int_s \frac{1}{2}\boldsymbol{u}^2 dr dz, \tag{5}$$

are introduced, where S is the integral region.

In this study, the radius ratio h is 0.667. The bulk of the results are obtained by the axisymmetric simulation, and some predictions are performed by the three-dimensional simulation in order to confirm the numerical results.

3. Results

3.1 Transient Developments of Flow Patterns

The main modes of the Taylor vortex flow are the primary mode, secondary normal mode and second anomalous mode (Koschmieder, 1993). The primary mode is the mode which appears first when the rotation speed gradually increases from rest, and it has an even number of cells. The flow is slowed down by the presence of the end wall and the retarded flow causes a normal cell which has an inward flow in the region adjacent to the end wall. The secondary normal mode has normal cells near end walls, but the number of cells is different from the one found in the primary mode. In the secondary anomalous mode, anomalous cell(s) appears on either or both end walls, and the number of cells is even or odd. Near the end wall, the anomalous cell has a flow directed outward which is opposite to the flow in the normal cell.

Figure 2 shows the time development of streamline plots (contours of y) of the flow at the aspect ratio 3.0 and the final Reynolds number 100. The value of y is zero on the walls, and the warm color and cold color represent positive values and negative values, respectively. The rotating inner cylinder is on the left side and the stationary outer cylinder is on the right side, and the upper and lower boundaries are end walls at rest. First cells form on the end walls. They gradually grow, and finally the two-cell mode appears.

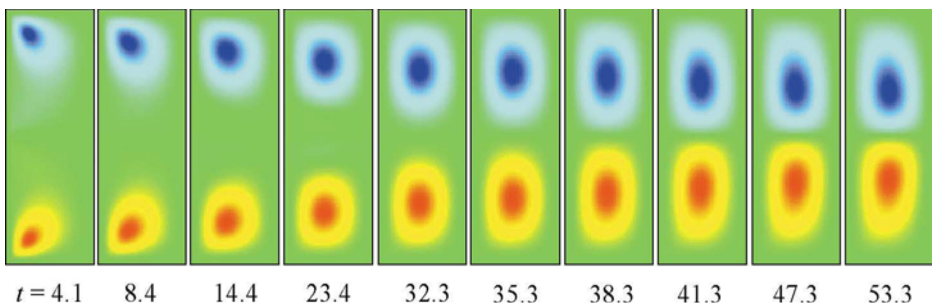

Fig. 2. Flow developing from end wall regions (G = 3.0, Re = 100).

Figure 3 illustrates the transition process to the anomalous four-cell mode at G= 4.0 and Re = 500. At t = 10.4, a pair of cells with outward flow between them grows around the mid-plane, and weak Ekman cells appear on end walls. Then some interior cells are induced. The Ekman cells are collapsed and the anomalous eight-cell mode is established (t = 29.0). The cell just below the mid-plane and the lower dominant cell approach each other and they merge into one cell, and so do the cell just above the mid-plane and the upper dominant cell (t = 49.8). The merged cell overlaps a small cell (t = 55.0), and the mode changes to the final four-cell mode.

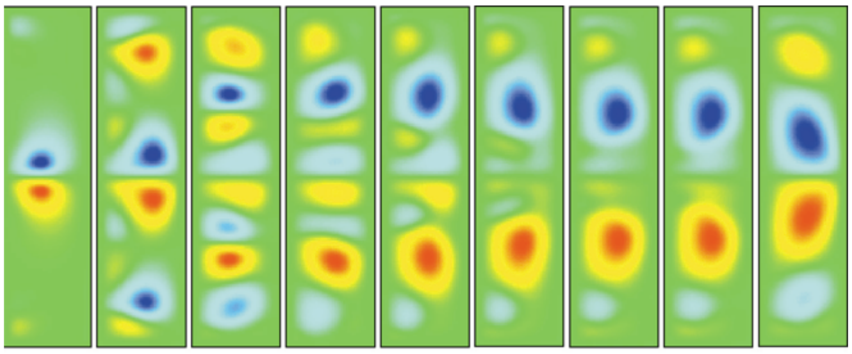

t = 10.4 21.5 29.0 36.4 43.9 49.8 53.5 55.0 66.2

Fig. 3. Flow development with overlapping cells around mid-plane (G = 4.0, Re = 500).

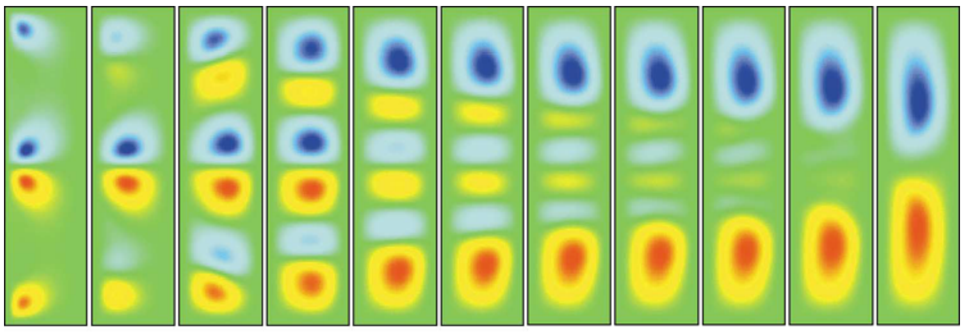

t = 9.4 15.7 22.0 91.2 169.9 217.1 248.6 258.0 264.3 270.6 276.9

Fig. 4. Flow development with decaying cells around mid-plane (G = 3.8, Re = 300).

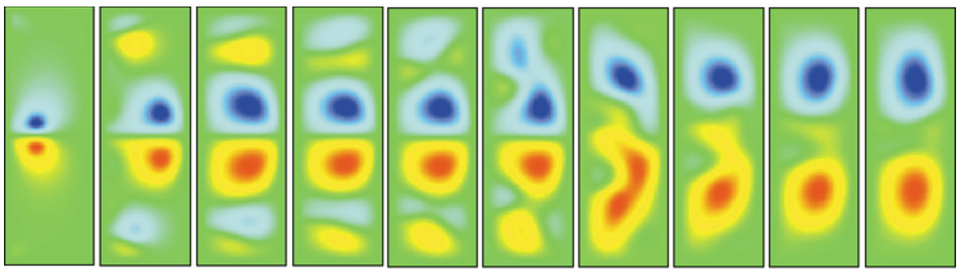

t = 7.2 19.1 114.7 215.1 222.3 227.1 231.9 234.3 236.7 239.0

Fig. 5. Flow development with overlapping cells around end walls (G = 2.8, Re = 800).

Some cells may decay before the final mode is established. Figure 4 shows the transition at G = 3.8 and Re = 300. First, four cells appear on end walls and around the mid-plane. Other cells are induced and the six-cell mode is formed (t = 22.0). Then four cells around the mid-plane in the axial direction gradually decay and the final flow of the two-cell mode appears.

Figure 5 shows the transition during which the cells on end walls merge with other cells. After the first cells appear around the mid-plane, the normal six-cell mode emerges (t = 215.1). Then the Ekman cells on end walls grow and they merge with interior cells which have the same sign of ψ (t = 227.1, 231.9). The merged cells overlap and collapse the cells with the opposite signs, and the final mode of the normal two cells is obtained.

The anomalous mode appears when the Ekman cells on end walls decay before the final mode is established. Figure 6 shows the transition at G = 3.8 and Re = 500. The first major cells emerge around the mid-plane and ten-cell mode appears, where the cells on end walls are too weak to be observable in the figure (t = 34.8).

Then the dominant cells merge with the cells around mid-plane and collapse the cells with opposite signs of y. After the six-cell mode forms (t = 56.4), the Ekman cells on end walls decay. The final mode of the flow is the anomalous four-cell mode in which the anomalous cells appear on end walls. An anomalous cell has two extra cells: one is between the inner cylinder and the end wall, and the other is between the outer cylinder and the end wall (Nakamura and Toya, 1996; Watanabe and Furukawa, 1999). The extra cells result from the decayed Ekman cell which is divided by the cell growing from the interior region.

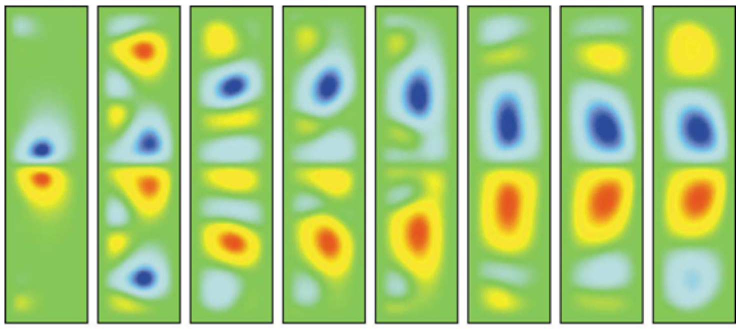

t = 10.8 22.8 34.8 40.8 46.8 56.4 70.8 108.0

Fig. 6. Flow development with decaying cells on end walls (G = 3.8, Re = 500).

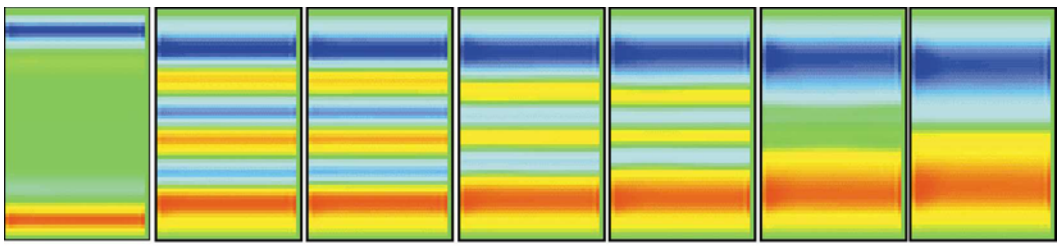

t = 11.3 47.2 53.0 56.2 59.8 66.1 73.3

Fig. 7. Contours of axial velocity component in radial plane (G = 3.0, Re = 300, $r - r_i$ = 0.025).

Figure 7 shows the time variation of the contours of the axial velocity component in the radial plane (q, z), which are obtained by the three-dimensional calculation. The upper and lower boundaries correspond to the end walls, and the axial direction z is vertical. The aspect ratio G is 3.0 and the Reynolds number Re is 300, and the radial section is at $r - r_i$ = 0.025. The first cells appear on the end walls (t = 11.3), and the six-cell mode is formed at an intermediate state (t = 47.2). Then the cells around the mid-plane disappear, and the final flow has the normal two-cell mode (t = 73.3). The profiles are almost constant in the circumferential direction. At higher Reynolds numbers, asymmetric patterns appeared during the transient processes, even though the final mode flows were practically axisymmetric.

3.2 Mean Energy

Time variations of the mean kinetic energy E are shown in Fig. 8. The initial flow is at rest, and the energy suddenly increases from zero. The energy of the flow at the aspect ratio 3.0 and the Reynolds number 100 grows monotonically and reaches its plateau after a small overshoot of its value. At G = 4.0 and Re = 500, a peak of value appears in the profile while the merged cells overlap weak cells and the eight-cell mode changes to the four-cell mode. In the flow at G = 3.8 and Re = 300, some cells disappear around the mid-plane. At the time when almost all the decaying cells disappear and the Ekman cells grow rapidly, the energy profile has its maximum. At G = 2.8 and Re = 800, the energy fluctuates before the final mode is established. We observed that the sizes of the major cells increased or decreased during the fluctuation of the energy. However, no correlation between the energy profile and the flow pattern was found. The flow at G = 3.8 and Re = 500 has the maximum of the energy when the Ekman cells are almost collapsed and the interior cells grow rapidly. In the present calculation, the energy peaks during transitions appeared when the final modes were almost established.

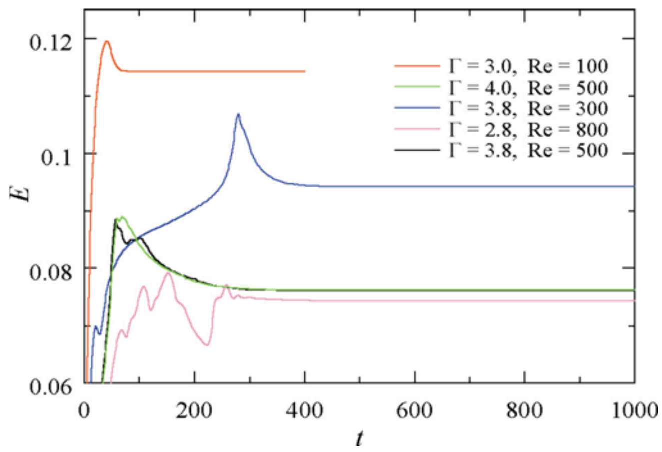

Fig. 8. Time variation of mean kinetic energy of the flows shown in Figs. 2-6.

4. Discussion

There are two major groups of developing processes. In the first group, the Ekman cell formed by the secondary flow on the end wall grows first. In the second group, a pair of cells first grows around the mid-plane. An experimental evidence suggests that the Ekman cells from the end walls do not invoke Taylor vortex flow and, as the centrifugal effect grows, the radial flow dominates before the secondary flow on the end wall gains strength (Takeda et al., 1990). As shown in Figs. 3-6, the result of the present calculation supports the experimental observation.

Flows in the second group are further classified according to the reduction way of the number of cells just before the final mode appears. The number of cell decreases when a dominant cell overlaps and collapses a small cell or when a weakening cell decays. The rough sketch of the decreasing process of the cell number is shown in Fig. 9. It represents the contour of stream function in the meridional section. The dominant cell and the vanishing

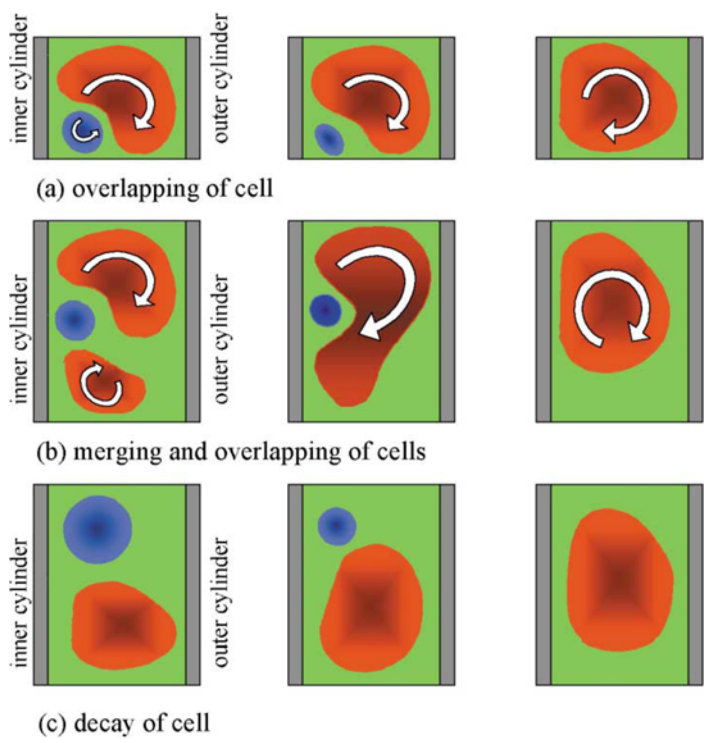

Fig. 9. Reduction of number of cells.

cell are side-by-side, and the rotating directions of them are opposite to each other. Figure 9(a) shows the process in which the dominant cell overlaps the vanishing cell and then collapses it. Figure 9(b) exhibits the way in which two co-rotating cells merge into one cell, and the small cell is overlapped and collapsed by the merged cell. Figure 9(c) shows the process in which the small cell decays and the dominant cell further grows. Hereafter, the reduction of the number of cells shown in Figs. 9(a) and (b) is called an overlapping reduction, and the cell reduction in Fig. 9(c) is called a decaying reduction.

The types of developing process are summarized in Table 1. In this table, an integer n represents a normal n-cell mode and An denotes an anomalous n-cell mode. In the present study, the developing processes of flows have six types:

Type 1: The first dominant cell which appears after the sudden start of rotation is the Ekman cell on the end wall of cylinders. As the Ekman cell grows, some cells are induced from the region near the end wall to the region around the mid-plane, and the number of cells increases monotonically. The Ekman cell has the inward flow near the end wall, and the final flow mode is normal.

Type 2: Before the final mode is attained, the overlapping reduction occurs around the mid-plane.

Type 3: Before the final mode is attained, the decaying reduction occurs around the mid-plane.

Type 4: Before the final mode is attained, the Ekman cell on the end wall is overlapped and collapsed.

Type 5: Before the final mode is attained, the Ekman cell on the end wall weakens and it divides into extra cells.

Type 6: The reduction of the cell number occurs neither around the mid-plane nor on the end wall.

Table. 1. Types of flow development.

Re \ Γ	2.8	3.0	3.2	3.4	3.8	4.0	4.2	4.4	4.6	4.8	5.0
800	2 (Type4)	2 (Type2)	A4 (Type2)	A4 (Type5)	A4 (Type5)	A4 (Type5)	4 (Type6)	6 (Type6)	6 (Type6)	6 (Type4)	6 (Type4)
700	2 (Type4)	A4 (Type5)	A4 (Type2)	2 (Type2)	A4 (Type5)	A4 (Type5)	A4 (Type5)	6 (Type4)	6 (Type4)	6 (Type4)	6 (Type4)
600	2 (Type3)	A4 (Type5)	A4 (Type5)	A4 (Type2)	4 (Type4)	4 (Type6)	6 (Type4)	6 (Type4)	6 (Type4)	6 (Type4)	6 (Type4)
500	A4 (Type5)	A4 (Type5)	2 (Type3)	2 (Type2)	A4 (Type5)	A4 (Type2)	A4 (Type5)	6 (Type4)	2 (Type2)	A6 (Type2)	6 (Type4)
400	2 (Type3)	A4 (Type5)	A4 (Type5)	A4 (Type5)	4 (Type3)	6 (Type4)	6 (Type4)	6 (Type6)	A4 (Type3)	A4 (Type2)	A6 (Type2)
300	2 (Type3)	2 (Type3)	2 (Type3)	2 (Type3)	2 (Type3)	4 (Type6)	6 (Type1)	6 (Type6)	6 (Type4)	6 (Type6)	6 (Type6)
200	2 (Type1)	2 (Type3)	2 (Type3)	2 (Type3)	2 (Type3)	2 (Type3)	4 (Type6)	6 (Type1)	6 (Type1)	6 (Type1)	6 (Type1)
100	2 (Type1)	2 (Type1)	2 (Type1)	2 (Type3)	4 (Type1)	4 (Type1)	4 (Type1)	4 (Type1)	4 (Type1)	4 (Type1)	6 (Type1)

Legend: Type1, Type2, Type3, Type4, Type5, Type6

Types 1-5 correspond to the flow developments shown in Figs. 2-6, respectively. The flow of Type 1 appears at relatively small Reynolds numbers. The flow of Type 6 is not clearly classified into Types 1-5 by our calculation.

5. Conclusion

The developing process of flow between two concentric rotating cylinders has been examined, and the developing processes of flows, which are difficult to investigate experimentally, have been clarified by the visualization of numerical results. The length of cylinder is finite and the inner cylinder suddenly starts to rotate. While the Ekman cells on end walls appear first at low Reynolds numbers, the cells formed by the centrifugal effect emerge first at higher Reynolds numbers. The formation processes to the final modes are classified into five types according to the position where first cell appears, the way of the reduction of the number of cells (overlapping or decaying) and the position where the reduction of the cell number occurs. When an anomalous mode appears, the Ekman cell on the end walls is divided by the cell growing from the mid-plane side, and the divided cells remain as extra cells on the end walls.

References

Benjamin, T. B. and Mullin, T., Anomalous Modes in the Taylor Experiment, Proceedings of the Royal Society of London, Series A, 377 (1981), 221-249.

Bielek, C. A. and Koschmieder, E. L., Taylor Vortices in Short Fluid Columns with Large Radius Ratio, Physics of Fluids A, 2-9 (1990), 1557-1563.

Egbers, C. and Pfister, G. (eds.), Physics of Rotating Fluids, (2000), Springer-Verlag.

Hirshfeld, D. and Rapaport, D. C., Molecular Dynamics Simulation of Taylor-Couette Vortex Formation, Physical Review Letters, 80-24 (1998), 5337-5340.

Koschmieder, E. L., Béard Cells and Taylar Vortices, (1993), Cambridge University Press.

Kuo, D. C. and Ball, K. S., Taylor-Couette Flow with Buoyancy: Onset of Spiral Flow, Physics for Fluids, 9 (1997), 2872-2884.

Lücke, M., Mihelcic, M. and Wingerath, K., Flow in a Small Annulus between Concentric Cylinders, Journal of Fluid Mechanics, 140 (1984), 343-353.

Nakamura, I., Toya, Y., Yamashita, S. and Ueki, Y., An Experiment on a Taylor Vortex Flow in a Gap with a Small Aspect Ratio (Bifurcation of Flows in a Symmetric System), JSME International Journal, Series II, 33-4 (1990), 685-691.

Nakamura, I. and Toya, Y., Existence of Extra Vortex and Twin Vortex of Anomalous Mode in Taylor Vortex Flow with a Small Aspect Ratio, Acta Mechanica, 117 (1996), 33-46.

Takeda, Y., Kobashi, K. and Fischer, W. E., Observation of the Transient Behaviour of Taylor Vortex Flow between Rotating Concentric Cylinders after Sudden Start, Experiments in Fluids, 9 (1990), 317-319.

Watanabe, T. and Furukawa, H., Mode Formation and Bifurcation in Decelerating Taylor Vortex Flow, Proceedings of the 3rd ASME/JSME Joint Fluids Engineering Conference (San Francisco), (1999), FEDSM99-6970.

Author Profile

Takashi Watanabe: He received his Ph.D. degree (Eng.) from Nagoya University in 1986. He now works as a professor at the Center for Information Media Studies, Nagoya University. His current research interests are the computational fluid dynamics of rotating flows and the human-computer interfaces. He is a member of the Japan Society of Mechanical Engineers, the Japan Society of Fluid Mechanics and the Japanese Society for Artificial Intelligence.

Hiroyuki Furukawa: He received the BE degree in Mechanical Engineering from Nagoya University (1997) and the MA degree in Human Informatics from Nagoya University (1999). He majors in Computational Fluid Dynamics as a Ph.D. candidate in Nagoya University. His researches include flow transient, flow visualization and non-linear dynamics.

Masae Aoki: She graduated from Faculty of Technology, Tokyo University of Agriculture and Technology in 1999, and received her Master of Arts from Nagoya University in 2001. Her master thesis is on the numerical analysis of the transient mechanism found in complex flows.

Ikuo Nakamura: He received his MSc.(Eng.) degree in Mechanical Engineering in 1959 from Nagoya University. He also received his Dr.Eng degree from the university in 1968. After working in Nissan Mo. Co. he has been a member of Mechanical Engineering Department of Nagoya University. He worked as a professor of fluids engineering of that department, mainly studying turbulent flow. Now he is a professor emeritus of Nagoya University and also a professor of Mechanical Engineering of Meijo University. His research interests are qualitative physical aspect of vortex in the sense of artificial intelligence and the diffusion in Taylor vortex.